

Accepted Manuscript

Negative permittivity adjusted by SiO₂-coated metallic particles in percolative composites

Peitao Xie, Kai Sun, Zhongyang Wang, Yao Liu, Runhua Fan, Zidong Zhang, Gerhard Schumacher

PII: S0925-8388(17)31458-5

DOI: [10.1016/j.jallcom.2017.04.248](https://doi.org/10.1016/j.jallcom.2017.04.248)

Reference: JALCOM 41652

To appear in: *Journal of Alloys and Compounds*

Received Date: 23 March 2017

Revised Date: 20 April 2017

Accepted Date: 22 April 2017

Please cite this article as: P. Xie, K. Sun, Z. Wang, Y. Liu, R. Fan, Z. Zhang, G. Schumacher, Negative permittivity adjusted by SiO₂-coated metallic particles in percolative composites, *Journal of Alloys and Compounds* (2017), doi: 10.1016/j.jallcom.2017.04.248.

This is a PDF file of an unedited manuscript that has been accepted for publication. As a service to our customers we are providing this early version of the manuscript. The manuscript will undergo copyediting, typesetting, and review of the resulting proof before it is published in its final form. Please note that during the production process errors may be discovered which could affect the content, and all legal disclaimers that apply to the journal pertain.



Negative Permittivity Adjusted by SiO₂-Coated Metallic Particles in Percolative Composites

Peitao Xie ^{a,b}, Kai Sun ^a, Zhongyang Wang ^{a,b}, Yao Liu ^{a,*}, Runhua

Fan ^{a,b}, and Zidong Zhang ^a, Gerhard Schumacher ^c

^a Key Laboratory for Liquid-Solid Structural Evolution and Processing of Materials (Ministry of Education), Shandong University, Jinan 250061, China

^b Dezhou META Research Center for Innovative Materials, Dezhou 253000, China

^c Helmholtz-Zentrum Berlin für Materialien und Energie GmbH, Hahn-Meitner Platz 1, D-14109 Berlin, Germany

*Corresponding author, E-mail: liuyao@sdu.edu.cn

Abstract

Negative permittivity has taken off as a research topic recent years in percolative composites. However, how to effectively tune the negative permittivity is still a challenge remained unsolved. Herein, the percolative composites with SiO₂-coated metallic particles homogeneously dispersed in epoxy resin were prepared using blending and hot-molding procedure. The negative permittivity was realized with the form of three-dimensional metallic network, and the value and frequency range of negative permittivity were precisely adjusted by the distribution of coated particles.

The analysis of Drude model indicated that negative permittivity was attributed to low frequency plasmonic state from the dilution of electron concentration. Moreover, coated particle can also change conductive path of electrons in composite, leading to an unusual linear relationship between conductivity and filler content, which is further certified by the equivalent circuit analysis. Our reported work would facilitate applications of negative permittivity materials especially in electromagnetic shielding, absorbing, attenuation and so on.

Keywords: Amorphous Alloy; Metal-Containing Polymer; Negative Permittivity; Intrinsic Metamaterials.

1.Introduction

Materials with negative electromagnetic parameters have taken off as a research topic due to their interesting properties and novel potential applications (first achieved in metamaterials). [1-3] It is worth to point out that the property of metamaterials is fundamentally dependent on the geometry of the artificial array structures rather than originating from its component materials.[4] In fact, it is further found that, even without artificial array structure, negative electromagnetic parameters can also be realized by the intrinsic property of component materials in the traditional percolative materials. Accordingly, these materials are also called intrinsic metamaterials or a

new concept “metacomposites”. [5-8]

In recent years, intrinsic metamaterials with tunable negative permittivity begin to gain extensive research attention due to the potential application, such as plasmons biosensing[9], microwave funneling[10], and electromagnetic shield[11], sensors[12-14], negative permittivity materials can also be used in left-handed materials when combined with negative permeability materials, etc. [15-17] However, the recent investigations of negative permittivity mainly focus on how to explain and realize negative permittivity. Theoretically, the negative permittivity can be obtained in percolative composites near or beyond the percolation threshold, attributed to plasma oscillation of delocalized electrons, following the Drude model’s description. [18] Based on the Drude-type response of CNFs, Zhong et al. [19] pioneered negative permittivity experimental work in the polymer nanocomposite with continuous 3D CNFs networks. Fan et al. [20,21] studied the negative permittivity in metal-ceramics composites with metallic conductive paths by a wet impregnation method. Besides, Qiu [22-24] and Guo[25,26] did excellent investigations to obtain negative permittivity in polyaniline matrix composites with the connectivity of different carbon materials.

As we can see, negative permittivity can be achieved by the connectivity of conductive fillers. However, there are few investigations paid close attention to the

value of negative permittivity which is crucial to application for different field. In fact, negative permittivity with small value is preferable in some instances. For example, negative permittivity with small value is required for impedance matching with negative permeability materials. [27] And negative permittivity with small value must be satisfied to excite surface plasma polarization for noble metal particles when used as biosensing at optical spectrum.[9] Besides, the capacitance enhancement, which is significant for miniaturization of electronic component, would be remarkable especially when the negative permittivity matches with positive permittivity based on the principle of series capacitor.[28,29] Therefore, the investigation of adjusting the value of negative permittivity is significant for theoretical research and application.

Herein, in order to get a better understanding of the relationship between the value of negative permittivity and metallic filler distribution, we propose a facile strategy to design such a composite with SiO₂-coated and uncoated metallic particles dispersed in epoxy matrix. Epoxy resin was chosen because of its good electric insulativity. To eliminate the impact of phase composition, the typical isotropic Fe₇₈Si₁₃B₉ (FeSiB) amorphous alloy particles were chosen as metallic fillers.

2.Experimental methods

Chemicals: Amorphous $\text{Fe}_{78}\text{Si}_{13}\text{B}_9$ (FeSiB) ribbons are purchased from Qingdao Yunlu Energy Technology Co. Ltd.. Sodium silicate (Na_2SiO_3), ethanediol and sulfuric acid (H_2SO_4) are purchased from Sinopharm Chemical Reagent Co. Ltd. China. Bisphenol A type solid epoxy resin is purchased from Shanghai Yoo-Pont Chemical Industry Co., LTO and used because of its good electric insulativity, chemical stability and easy processing.[30-32] The chemicals are obtained as chemically pure grade products and used without any further treatment.

The Preparation of $\text{Fe}_{78}\text{Si}_{13}\text{B}_9$ Powders: Embrittlement treatment is carried out in a tubular resistance furnace with argon atmosphere at $300\text{ }^\circ\text{C}$ for one hour. After cut into pieces with scissor, the ribbons are put into the ball mill pot, and grinding is operated by cryomilling at liquid nitrogen temperature to avoid crystallization in the process of high-energy ball mill. Finally, the powders size is controlled by sieving through 100-mesh and 150-mesh sieve.

The Fabrication of Coated $\text{Fe}_{78}\text{Si}_{13}\text{B}_9$ Powders: The FeSiB powders are mixed with ethanediol with mass ratio of 1:50, and the suspension is obtained after ultrasonic dispersion for 60 min. Then, the suspension is transferred to a water bath thermostat at $90\text{ }^\circ\text{C}$ with mechanical force stirring. The Na_2SiO_3 solution of 1mol/L and H_2SO_4 solution of 1mol/L are simultaneously added into the suspension at the speed of 200

mL/h. Keep stirring for 2 hours, and the coated FeSiB powders are obtained after filtration and drying. The coating of the powders with this process is amorphous SiO₂.

The Fabrication of Fe₇₈Si₁₃B₉/Epoxy Composites: There are two kinds of FeSiB powders. One is the coated by a thin insulative SiO₂ layer, named coated FeSiB powder; the other is uncoated FeSiB powder with normal conductivity. FeSiB powder was uniformly mixed with epoxy powder by cryomilling. The mixed powder is processed into bulk composites by hot compression molding. The FeSiB/Epoxy composites with different uncoated FeSiB content and coated-FeSiB/Epoxy composites with different coated-FeSiB content are fabricated, denoted as FeSiB_xEpoxy_{1-x} and coated-FeSiB_xEpoxy_{1-x} ($0 \leq x \leq 1$), respectively. Besides, the epoxy resin powder is kept 40 % volume fraction, and the hybrid composites are prepared after uniformly mixing the two different metallic filler with epoxy resin powder. The hybrid composites are denoted as (FeSiB_xcoated-FeSiB_{1-x})_{0.6}Epoxy_{0.4} ($x=0.7-1$), where the x is the ratio of SiO₂-coated and uncoated FeSiB. The microstructure was observed by scanning electron microscopy. The phase compositions were investigated by X-ray diffraction (XRD). The dielectric properties of the composites at the frequency range from 10 MHz to 1 GHz were tested by Agilent E4991A precision impedance analyzer equipped with 16453A test fixture. The samples dimension is ϕ 20 mm \times 2 mm for permittivity test. [21]

3.Results and Discussion

3.1Microstructure

Fig. 1(a) shows SEM images and EDX results of one SiO₂-coated FeSiB particle inlaid into resin after polished with EDX results. It is indicated the coating was SiO₂ with the thickness of 1.5 μm. Fig. 1(b) is the SEM images of fractured surface after polished for composites with 60 % volume fraction FeSiB content. The particles contacted with each other in the composite with 60 vol% FeSiB, and percolating network can form, which is illustrated by the solid lines.

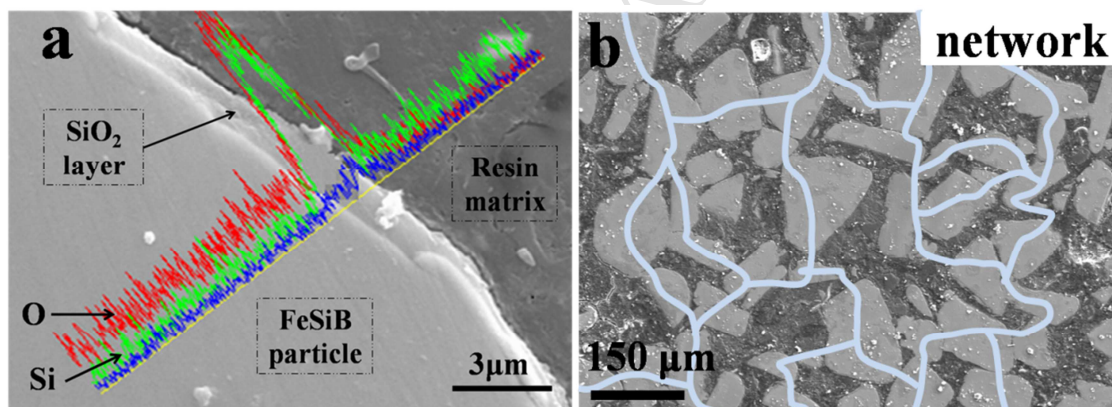


Fig. 1 SEM images and EDX results of one SiO₂-coated FeSiB particle inlaid into resin after polished (a), and fractured surface after polished for composites with 60 % volume fraction FeSiB content (b). The solid lines in (b) illustrated the network formed by FeSiB particles.

3.2Negative permittivity behavior

It is concluded from the Fig. S4 in Supplementary Information that, the uncoated FeSiB particles could act as conductive filler leading to negative permittivity, the

SiO₂-coated FeSiB particles could work as insulative filler generating positive permittivity. In order to further tune the negative permittivity, the composites with different ratio of Fe and coated-Fe are prepared and the frequency dispersion of ϵ_r' is investigated in the Fig. 2. The ϵ_r' of hybrid composites with $x=0.7, 0.8$ takes positive value, turns to negative for $x=0.85, 0.9, 0.95, 1$. Although the FeSiB content keeps at 60% volume fraction, the ϵ_r' for the hybrid composites shows a dual percolative behavior with the change of coated and uncoated particle ratio. Similar results were also discovered in Ni_{0.3}Zn_{0.7}Fe_{1.95}O₄-Ni-Polymer composite [33], which was attributed to the different electrical property of the two different fillers. Compared with results in Fig.S4, the results above are clearly shown that the addition of coated metallic particle not only contributes the negative permittivity with small value but also adjusted its frequency range. Moreover, negative permittivity behavior can be described by Drude model: [34]

$$\epsilon_r' = 1 - \frac{\omega_p^2}{\omega^2 + \omega_\tau^2} \quad (1)$$

$$\omega_p = \sqrt{\frac{n_{eff} e^2}{m_{eff} \epsilon_0}} \quad (2)$$

$$\omega_0 = \sqrt{\omega_p^2 - \omega_\tau^2} \quad (3)$$

where ω_τ is the damping constant, $\omega_p = 2\pi f_p$ is plasmons angular frequency, ω is angular frequency of applied electric field, n_{eff} is effective concentration of electron,

m_{eff} is effective weight of electron, and ϵ_0 is vacuum permittivity (8.85×10^{-12} F/m).

The ω_0 is a derived parameter, corresponding to the characteristic frequency $f_0 = \omega_0/2\pi$, where $\epsilon_r' = \text{zero}$. The solid line in Fig. 3 is the fitting result for FeSiB_{0.6}Epoxy_{0.4} composite using the Equation (1), agreeing well with the experimental data with the $f_p = 2.19$ GHz, the reliability factor $R^2=0.9892$. Hence, the f_p of other hybrid composites is below 2.19 GHz (usually at optical or ultraviolet frequency region for metals). The red shift of f_p indicates the low frequency plasmons state which was theoretically proposed by Pendry[35] in metallic mesostructures in 1996 and then extensively investigated in intrinsic metamaterials. Tsutaoka *et al.* studied the low frequency plasmons state in Cu granular composites ($f_p \approx 10\text{-}1000$ GHz) [34] and Fan *et al.* in nano-sized Ni ($f_p = 27$ GHz)[36], Ag (16 GHz) [20] and Fe (208 GHz) [21] particle composites. According to the Equation (3), the red shift of f_p would lead to low frequency f_0 (inset of Fig. 2), which led to the tunable negative permittivity with different value and frequency range.

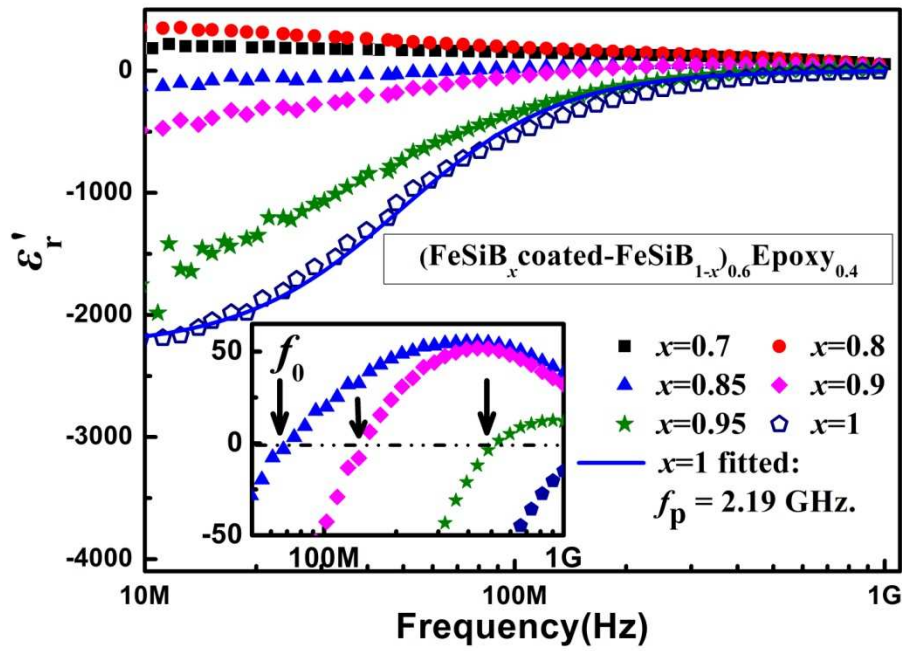


Fig. 2 The frequency dispersion of ϵ'_r for hybrid composites $(\text{FeSiB}_x \text{ coated-FeSiB}_{1-x})_{0.6} \text{Epoxy}_{0.4}$.

The solid line showed the fitting result by Drude model. The inset showed the local enlarged view at high frequency range.

3.3 Conductivity and percolation

The different frequency dispersion of ac conductivity σ_{ac} of the composites clearly indicated a percolative phenomenon (Fig. 3a). Below the percolation threshold ($x=0.7, 0.8$), σ_{ac} has an exponential relationship with frequency, following the power law [37] $\sigma_{ac} \propto \omega^n$ ($0 < n < 1$). The fitting result is also given (Fig. 3a) and agrees well with the experimental data, indicating a hopping conductive behavior. Above the percolation threshold, with the formation of percolative conductive network, the decreasing trend of σ_{ac} was attributed to the skin effect at high frequency, which could be described by skin depth[38]: $\delta = \sqrt{2/\omega\sigma\mu}$, where δ is the skin depth, σ the dc conductivity, μ the

static permeability. The skin depth (conductive cross section) gradually reduces, leading to the decreasing of conductivity.

Fig. 3(b) is the relationship between σ_{ac} at 80 MHz and the filler ratio for the composites $(\text{FeSiB}_x\text{-coated-FeSiB}_{1-x})_{0.6}\text{Epoxy}_{0.4}$. As shown in the Fig. 3(b), unlike the usual ladder-shape transition tendency in other percolative composite [37-39], a novel linear relationship between σ_{ac} and uncoated FeSiB filling ratio is observed above percolation threshold, which is attributed to the change of microstructure in the hybrid composites (schemed in the inset of Fig. 3b). With increasing the coated FeSiB ratio, the insulative SiO_2 layer would gradually and uniformly cut off the conductive paths. That is to say, the tunable conductive network leads to the novel conductive property based on the carrier concentration: [40-42] $\sigma \propto n$. Although the free electron concentration of total fillers remains constant in the composites as the total FeSiB content keeps at 60% volume fraction, the electrons in the coated particles are localized by the SiO_2 layer no long “free”, leading to the decrease of effective carrier concentration. Hence, according to equation (2), the low effective carrier concentration leads to the low frequency plasmons state at radio-frequency range, near where negative permittivity of small value could be achieved. Similar results were also discovered in plasmons materials at infrared frequency range, whose surface and bulk plasmons resonance frequency could also be adjusted by carrier

concentration. [43] By strictly controlling the ratio of coated and uncoated filler, the ac conductivity and negative permittivity show a feasible tunability compared to our early study work. [20,21,36]

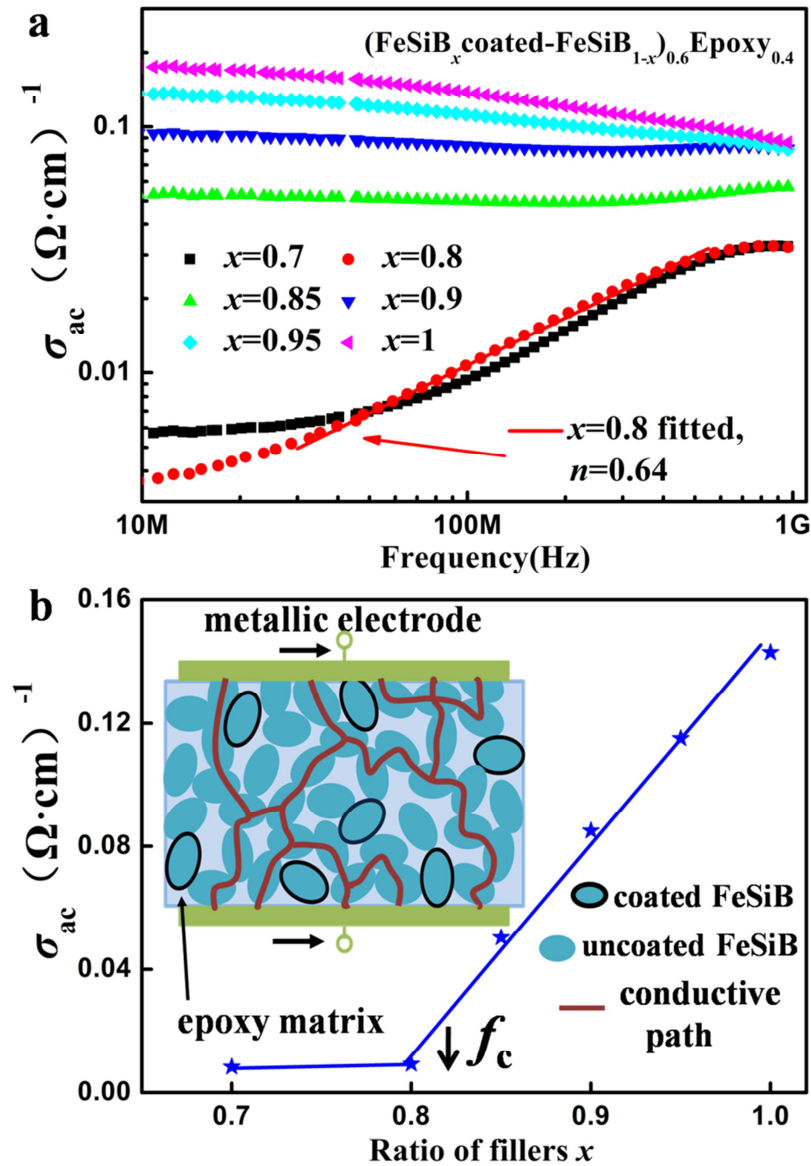


Fig.3 The frequency dispersion of ac conductivity σ_{ac} (a), the relationship between σ_{ac} at 80 MHz and ratio of fillers for the hybrid composites $(\text{FeSiB}_x\text{coated-FeSiB}_{1-x})_{0.6}\text{Epoxy}_{0.4}$ (b). The inset in (b) showed the schematic diagram of microstructure variation in the composites with the addition of coated particles.

3.4 Impedance and equivalent circuit

Fig. 4 shows the frequency dispersion of reactance Z'' for the composites $(\text{FeSiB}_x\text{coated-FeSiB}_{1-x})_{0.6}\text{Epoxy}_{0.4}$. For hybrid composites of $x=0.7, 0.8$, the reactance takes negative value, indicating capacitive behavior. For composites of $x=0.85, 0.9, 0.95$, the reactance takes positive value at lower frequency range but turns to negative at higher frequency range. Interestingly, the positive-negative switching phenomenon for Z'' corresponded well to negative-positive switching for ϵ_r' . For the composite of $x=1$, the reactance kept positive over the whole frequency range, suggesting the inductive character.

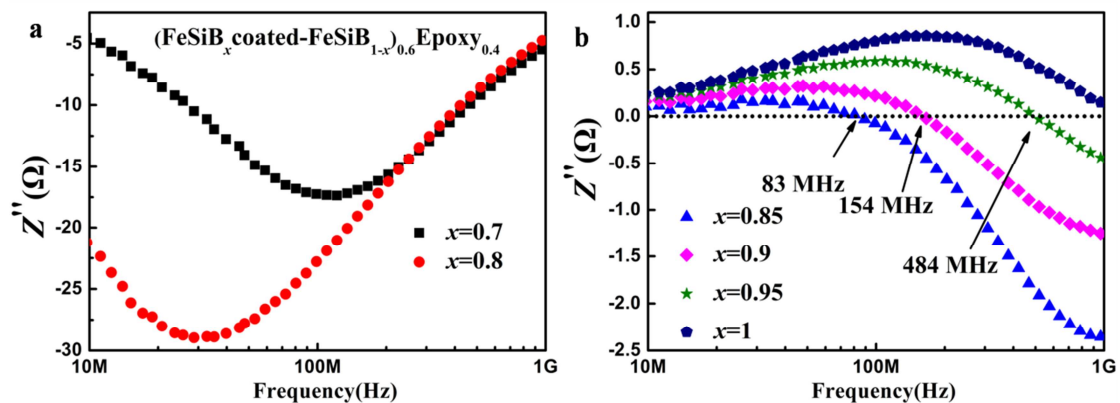


Fig.4 The frequency dispersion of impedance for the composites $(\text{FeSiB}_x\text{coated-FeSiB}_{1-x})_{0.6}\text{Epoxy}_{0.4}$.

The equivalent circuit analysis is performed to further investigate the impedance property (Fig. 5 and Table 1). Below percolation threshold, the composites could be equivalent into a circuit by a series resistor R_s and a parallel connection of a resistor R_p and a capacitor C_p (Fig. 5a). The R_s comes from the silver electrode with a small

value. The R_p results from the leakage current due to the mutual contact or agglomeration of fillers. Above percolation threshold, it is showed that shunt inductors always exist for the composites with negative permittivity behavior (Fig.5b). For the the composites of $x=1$, three inductors exist, while two inductors for $x=0.95$ and only one inductor for $x=0.85$. As known, inductor indicates the existence of conductive path; the decrease of inductor number could be attributed to the cut-off conductive paths (Fig. 3b). Indeed, in the right/left-handed transmission line metamaterials, the negative permittivity was achieved by the shunt inductors, and the increase of the inductor number indicated more contribution to the negative permittivity. [44,45] Therefore, when the ratio of SiO_2 -coated particle is controlled above but near the percolation threshold in the composites, the decreasing of inductor number contributed to the smaller value of negative permittivity.

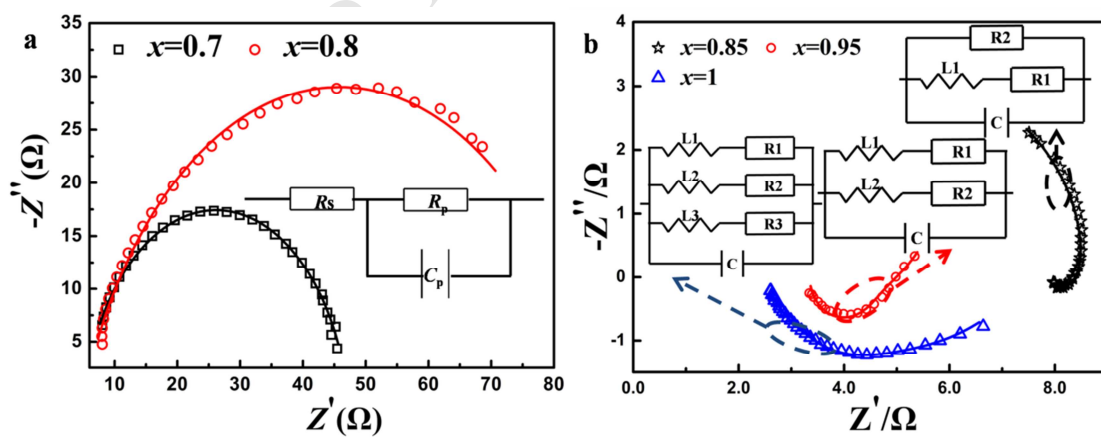


Fig.5 Nyquist plot for the composites $(\text{FeSiB}_x\text{-coated-FeSiB}_{1-x})_{0.6}\text{Epoxy}_{0.4}$. The solid lines in (a) and (b) are fitting results using equivalent circuit.

Table 1 The corresponding parameters of the simulating results by equivalent circuit

analysis for the composites (FeSiB_xcoated-FeSiB_{1-x})_{0.6}Epoxy_{0.4}.

Value of x	$R_s(\Omega)$	$R_p(\Omega)$	$C(\text{pF})$	$L_1(\text{nH})$	$R_1(\Omega)$	$L_2(\text{nH})$	$R_2(\Omega)$	$L_3(\text{nH})$	$R_3(\Omega)$
0.7	7.12	37.21	34.76						
0.8	8.26	60.86	43.42						
0.85			8.89	103.21	36.18		6.13		
0.95			17.93	28.94	11.94	0.36	4.67		
1			15.01	51.22	11.76	9.39	9.39	0.50	5.15

5. Conclusions

In summary, the materials with tunable negative permittivity are realized by controlling the distribution of SiO₂-coated and uncoated FeSiB particles in insulative resin matrix. Negative permittivity is attributed to the low frequency plasmons state which could be adjusted by the dilution of effective carrier concentration. The insulative SiO₂ coating by chemical modification changes the movement of free electrons among metallic fillers and the electrical connectivity of fillers. The weak connectivity of conductive filler leads to the small value of negative permittivity, which is further verified by the decrease of inductor number in equivalent circuit. The exploration of tunable negative permittivity would have significance on the intrinsic metamaterials and novel potential applications, especially in lossy material and capacitance enhancement.

Acknowledgement

This study was financially supported by the National Natural Science Foundation of China [grant No.51402170], Postdoctoral Science Foundation of China [grant No. 2014M551900] and Shandong Provincial Natural Science Foundation, China [grant No. ZR2013EMQ010], [grant No. ZR2016EMM09].

References

- [1] T. Tsutaoka, H. Massango, T. Kasagi, Yamamoto, and K. Hatakeyama, *Appl. Phys. Lett.*, 2016, 108(19): 191904.
- [2] R. Yahiaoui, H. Němec, P. Kužel, F. Kadlec, C. Kadlec, and P. Mounaix, *Opt. Lett.*, 2009, 34(22): 3541-3543.
- [3] R. A. Shelby, D. R. Smith, S. Schult. *Science* 292, 77 (2001).
- [4] W. A. Murray, W. L. Barnes, *Adv. Mater.*, 2007, 19(22): 3771-3782.
- [5] J. Zhu, S. Wei, L. Zhang, Y. Mao, J. Ryu, P. Mavinakuli, A. B. Karki, D. P. Young, and Z. Guo, *J. Phys. Chem. C*, 2010, 114(39): 16335-16342.
- [6] J. Zhu, S. Wei, L. Zhang, Y. Mao, J. Ryu, A. B. Karki, D. P. Young and Z. Guo, *J. Mater. Chem.*, 2011, 21(2): 342-348.
- [7] K. Sun, R. Fan, Y. Yin, J. Guo, X. Li, Y. Lei, L. An, C. Cheng, and Z. Guo, *J. Phys. Chem. C*, 2017, 121 (13), 7564–7571

- [8] H. Gu, J. Guo, M. A. Khan, D. P. Young, T. D. Shen, S. Wei and Z. Guo, *Phys. Chem. Chem. Phys.*, 2016, 18 (29).
- [9] Y. Wang, L. Wu, T. Wong, M. Bauch, Q. Zhang, J. Zhang, *Nanoscale*, 2016, 8(15): 8008-8016.
- [10] R. Liu, Q. Cheng, H. Thomas, J. Jack, T. Cui, S. Cummer and D. R. Smith, *Phys. Rev. Lett.*, 2008, 100(2): 023903.
- [11] A. Alù, N. Engheta, *Phys. Rev. E*, 2005, 72(1): 016623.
- [12] H. Liu, M. Dong, W. Huang, J. Gao, K. Dai, J. Guo, G. Zheng, C. Liu, C. Shen and Z. Guo, *J. Mater. Chem. C*, 2017, 5(1): 73-83.
- [13] H. Liu, J. Gao, W. Huang, K. Dai, G. Zheng, C. Liu, C. Shen, X. Yan, J. Guo and Z. Guo, *Nanoscale*, 2016, 8(26): 12977-12989.
- [14] H. Liu, Y. Li, K. Dai, G. Zheng, C. Liu, C. Shen, X. Yan, J. Guo and Z. Guo, *J. Mater. Chem. C*, 2016, 4, 157-166.
- [15] C. Alippi, *CAAI Transactions on Intelligence Technology*, 1, 1-3 (2016)
- [16] H. Jin, Q. Chen, Z. Chen, Y. Hu, J. Zhang, *CAAI Transactions on Intelligence Technology*, 1, 104-113 (2016).
- [17] X. Zhang, H. Gao, M. Guo, G. Li, Y. Liu, D. Li, *CAAI Transactions on Intelligence Technology*, 1, 4-13 (2016)
- [18] S. T. Chui, L. Hu, *Phys. Rev. B*, 2002, 65(14): 144407.

- [19] B. Li, G. Sui, W. H. Zhong, *Adv. Mater.*, 2009, 21(41): 4176-4180.
- [20] Z. C. Shi, R. H. Fan, Z. D. Zhang, H. Y. Gong, J. Ouyang, Y. J. Bai, X. H. Zhang, and L. W. Yin, *Appl. Phys. Lett.*, 2011, 99(3): 032903.
- [21] Z. C. Shi, R. H. Fan, K. Yan, K. Sun, M. Zhang, *Adv. Funct. Mater.*, 2013, 23(33): 4123-4132.
- [22] X. Yao, X. Kou, J. Qiu, *Carbon* 107 (2016) 261-267
- [23] X. Yao, X. Kou, J. Qiu, *Org. Electron.*, 2016, 38: 55-60.
- [24] X. Kou, X. Yao, J. Qiu, *Org. Electron.*, 2016, 38: 42-47.
- [25] H. Gu, J. Guo, Q. He, Y. Jiang, Y. D. Huang, N. Haldolaarachige, Z. P. Luo, D. P. Young, S. Y. Wei and Z. H. Guo, *Nanoscale*, 2014, 6(1): 181-189.
- [26] J. Guo, H. Gu, H. Wei, Q. Y. Zhang, N. Haldolaarachchige, Y. Li, D. P. Young, S. Y. Wei, and Z. H. Guo, *J. Phys. Chem. C*, 2013, 117(19): 10191-10202.
- [27] C. Kurter, T. Lan, L. Sarytchev, S. M. Anlage, *Phys. Rev. Appl.*, 2015, 3(5): 054010.
- [28] V. V. Zhirnov, R. K. Cavin, *Nat. Nanotechnol.*, 2008, 3(2): 77-78.
- [29] P. Zubko, J. C. Wojdeł, M. Hadjimichael, F. Stéphanie, S. Anaïs, L. Igor, J. Triscone and J. Íñiguez, *Nature*, 534, 524–528 (2016).
- [30] X. Cao, X. Wei, G. Li, C. Hu, K. Dai, J. Guo, G. Zheng, C. Liu, C. Shen, Z. Guo, *Polymer*, 2017, 112: 1-9.

- [31] H. Gu, C. Ma, J. Gu, J. Guo, X. Yan, J. Huang, Q. Zhang and Z. Guo, *J. Mater. Chem. C*, 2016, 4(25): 5890-5906.
- [32] H. Gu, J. Guo, H. Wei, S. Guo, J. Liu, Y. Huang, M. A. Khan, X. Wang, D. P. Young, S. Wei, Z. Guo, *Adv. Mater.*, 2015, 27(40): 6277-6282.
- [33] Y. Shen, Z. Yue, M. Li, C. W. Nan, *Adv. Funct. Mater.*, 2005, 15(7): 1100-1103.
- [34] T. Tsutaoka, T. Kasagi, S. Yamamoto, and K. Hatakeyama, *Appl. Phys. Lett.* 102, 181904 (2013).
- [35] J. B. Pendry, A. J. Holden, W. J. Stewart, I. Youngs, *Phys. Rev. Lett.* 76, 4773 (1996).
- [36] Z. Shi, R. Fan, Z. Zhang, L. Qian, M. Gao, M. Zhang, L. T. Zheng, X. H. Zhang and L. W. Yin, *Adv. Mater.* 24, 2349 (2012).
- [37] J. C. Dyre, T. B. Schrøder, *Rev. Mod. Phys.*, 2000, 72(3): 873.
- [38] X. Wang, Z. Shi, M. Chen, R. Fan, K. Yan, K. Sun, S. Pan, M. Yu, *J. Am. Ceram. Soc.*, 2014, 97(10): 3223-3229.
- [39] Z. M. Dang, Y. H. Lin, C. W. Nan, *Adv. Mater.* 15, 1625 (2003).
- [40] Z. Huang, X. Dai, Y. Yu, C. Zhou, F. Zu, *Scripta Mater.*, 2016, 118: 19-23.
- [41] L. D. Zhao, J. He, D. Berardan, Y. H. Lin, J. F. Li, C. W. Nan and N. Dragoe, *Energ. Environ. Sci.*, 2014, 7(9): 2900-2924.

[42] J. Q. Li, Z. W. Lu, S. M. Li, S. M. Li, F. S. Liu, W. Q. Ao, Y. Li, *Scripta Mater.*,

2016, 112: 144-147.

[43] A. Boltasseva, H. A. Atwater, *Science*, 2011, 331(6015): 290-291.

[44] C. Caloz *Mater. Today* 12, 12 (2009).

[45] F. Bongard, H. Lissek, J. R. Mosig. *Phys. Rev. B* 82, 094306 (2010).

1. Negative permittivity is precisely adjusted by the coated metallic particles.
2. An unusual linear relation between conductivity and filler content is obtained.
3. The impedance spectra are systematically investigated by the equivalent circuit.